Carcinogenesis vol.34 no.6 pp.1331–1342, 2013
doi:10.1093/carcin/bgt060
Advance Access publication February 7, 2013

Arenobufagin, a natural bufadienolide from toad venom, induces apoptosis and autophagy in human hepatocellular carcinoma cells through inhibition of PI3K/Akt/mTOR pathway

Dong-Mei Zhang[1,2,†], Jun-Shan Liu[1,2,†], Li-Juan Deng[1,2], Min-Feng Chen[1,2], Anita Yiu[3], Hui-Hui Cao[1,2], Hai-Yan Tian[1,2], Kwok-Pui Fung[3], Hiroshi Kurihara[1,2], Jing-Xuan Pan[4] and Wen-Cai Ye[1,2,*]

[1]Institute of Traditional Chinese Medicine and Natural Products, College of Pharmacy, Jinan University, Guangzhou 510632, China, [2]Guangdong Province Key Laboratory of Pharmacodynamic Constituents of TCM and New Drugs Research, Jinan University, Guangzhou 510632, China, [3]School of Biomedical Sciences, The Chinese University of Hong Kong, Hong Kong, China and [4]Department of Pathophysiology, Zhongshan School of Medicine, Sun Yat-Sen University, Guangzhou 510632, China

*To whom correspondence should be addressed. Tel: +86 20 8522 0936; Fax: +86 20 8522 1559;
Email: chywc@yahoo.com.cn
Correspondence may also be addressed to Jing-Xuan Pan. Tel/Fax: +86 20 8733 2788;
Email: panjx2@mail.sysu.edu.cn

Hepatocellular carcinoma (HCC) is a deadly form of cancer without effective chemotherapy so far. Currently, only sorafenib, a multitargeted tyrosine kinase inhibitor, slightly improves survival in HCC patients. In searching for natural anti-HCC components from toad venom, which is frequently used in the treatment of liver cancer in traditional Chinese medicine, we discovered that arenobufagin, a bufadienolide from toad venom, had potent antineoplastic activity against HCC HepG2 cells as well as corresponding multidrug-resistant HepG2/ADM cells. We found that arenobufagin induced mitochondria-mediated apoptosis in HCC cells, with decreasing mitochondrial potential, as well as increasing Bax/Bcl-2 expression ratio, Bax translocation from cytosol to mitochondria. Arenobufagin also induced autophagy in HepG2/ADM cells. Autophagy-specific inhibitors (3-methyladenine, chloroquine and bafilomycin A1) or Beclin1 and Atg 5 small interfering RNAs (siRNAs) enhanced arenobufagin-induced apoptosis, indicating that arenobufagin-mediated autophagy may protect HepG2/ADM cells from undergoing apoptotic cell death. In addition, we observed the inhibition of phosphatidylinositol 3-kinase (PI3K)/Akt/mammalian target of rapamycin (mTOR) pathway by arenobufagin. Interestingly, inhibition of mTOR by rapamycin or siRNA duplexes augmented arenobufagin-induced apoptosis and autophagy. Finally, arenobufagin inhibited the growth of HepG2/ADM xenograft tumors, which were associated with poly (ADP-ribose) polymerase cleavage, light chain 3-II activation and mTOR inhibition. In summary, we first demonstrated the antineoplastic effect of arenobufagin on HCC cells both *in vitro* and *in vivo*. We elucidated the underlying antineoplastic mechanisms of arenobufagin that involve cross talk between apoptosis and autophagy *via* inhibition of the PI3K/Akt/mTOR pathway. This study may provide a rationale for future clinical application using arenobufagin as a chemotherapeutic agent for HCC.

Abbreviations: ANOVA, analysis of variance; BA, bafilomycin A; CQ, chloroquine; Dox, doxorubicin; FITC, fluorescein isothiocyanate; HCC, hepatocellular carcinoma; JC-1, 5,5′,6,6′-tetrachloro-1,1′,3,3′-tetraethylbenzimidazolyl-carbocyanine iodide; LC3, light chain 3; 3-MA, 3-methyladenine; MDC, monodansylcadaverine; mTOR, mammalian target of rapamycin; MTT, 3-(4,5-dimethylthiazol-2-yl)-2,5-diphenyltetrazolium bromide; PARP, poly (ADP-ribose) polymerase; PBS, phosphate-buffered saline; PI, propidium iodide; PI3K, phosphatidylinositol 3-kinase; SEs, standard errors; siRNA, small interfering RNA; TCM, traditional Chinese medicine; TEM, transmission electron microscopy.

[†]These authors contributed equally to this work.

Introduction

Liver cancer ranks third among all cancer-related deaths, causing more than 662 000 deaths annually worldwide, about half of which occur in China (1,2). More than 80% of liver cancer is hepatocellular carcinoma (HCC), which originates from hepatocytes, the predominant type of cells in the liver. The etiology of HCC is principally associated with hepatitis B and C infection. Surgical resection is the treatment of choice but is suitable for only a small fraction of patients with localized foci. Liver transplantation can be an option. However, it is restricted due to the limited availability of donor livers. Systemic chemotherapy with doxorubicin (Dox), paclitaxol and cisplatin as monotherapy or in combination has shown modest efficacy with severe side effects. So far, only sorafenib, a multitargeted tyrosine kinase inhibitor, has been shown to significantly improve survival by a median of 3 months in HCC patients (3). Overall, although multiple modules of treatment including surgical resection and systemic or infusional chemotherapy have been applied, the overall 5 year survival rate for patients with liver cancer is <14% (4). Therefore, there is an urgent need for novel chemotherapeutic agents for the treatment of HCC.

Toad venom (venenum bufonis, also called Chan'su) is derived from the dried skin secretions of giant toads (*Bufo gargarizans* Cantor or *Bufo melanostictus* Suhneider) and has been widely used for centuries in traditional Chinese medicine (TCM) alone or in combination with other herbal ingredients. In fact, toad venom is currently used in clinical practice of TCM to treat HCC (5). Despite intensive efforts to identify the biologically active components of toad venom, the exact component(s) and the precise underlying mechanisms against tumor cells remain unclear (6–8). In our bioassay-guided isolation of anti-hepatoma constituents from toad venom, we discovered that arenobufagin possessed the most potent antitumor activity compared with 15 reported bufadienolides isolated from toad venom (9,10).

Cruz *et al.* (11,12) reported that arenobufagin blocks Na^+–K^+ pump current in cardiac myocytes like other cardiotoxic steroidal compounds (e.g. digitoxin, oleandrin and bufalin). It has recently been reported by our group that arenobufagin blocks vascular endothelial growth factor-mediated angiogenesis (13). Here, we reported the novel finding that arenobufagin induces apoptosis and autophagy *via* inhibition of the phosphatidylinositol 3-kinase (PI3K)/Akt/mammalian target of rapamycin (mTOR) pathway in HCC cells. Our findings suggested that arenobufagin could be a promising agent for the treatment of HCC.

Materials and methods

Reagents

Dox was purchased from Merck Calbiochem (San Diego, CA). Annexin V–fluorescein isothiocyanate (FITC)/propidium iodide (PI) apoptosis detection kit was supplied by Biouniquer Tech (Nanjing, China). 5,5′,6,6′-Tetrachloro-1,1′,3,3′-tetraethylbenzimidazolyl-carbocyanine iodide (JC-1) and Alexa Fluor 488-conjugated antirabbit IgG antibody were obtained from Invitrogen Molecular Probes (Guangzhou, China). Cyto-ID® Autophagy detection kit was purchased from Enzo Life Sciences (Farmingdale, NY). Antibodies used in western blot analysis were listed in Supplementary Table S1, available at *Carcinogenesis* Online. Akt small interfering RNA (siRNA) I kit was supplied by Cell Signaling (Beverly, MA). PI3K activator was purchased from Santa Cruz (Dallas, TX). Atg5, beclin 1 and mTOR siRNA kits were purchased from Genepharma (Shanghai, China). Protein inhibitor cocktail tablets were purchased from Roche Applied Science (Mannheim, Germany). Hematoxylin and eosin staining kit was purchased from Jiancheng Bioengineering Institute (Nanjing, China). Other chemicals were obtained from Sigma (St Louis, MO).

Extraction and isolation of arenobufagin

The toad venom (1.5 kg) was dried and powdered. Arenobufagin was extracted using 95% ethanol under ultrasonic conditions (40 min, 40°C) and then

concentrated under reduced pressure to yield a 900 g residue. The residue was subsequently partitioned between methylene dichloride and water. The methylene dichloride extract (321 g) was then subjected to chromatography with silica gel (200–300 mesh) and eluted with successive mixtures of cyclohexane–acetone (5:1, 3:1 and 1:1) to give 15 fractions (fraction 1–15). Fraction 6 was further subjected to reverse-phase C_{18} silica gel chromatography, eluted with methanol–water gradients (30:70–90:10) to obtain compound **1** (1.5 g). Compound **1** was identified as arenobufagin (Figure 1A) by comparing its spectrum data with parameters in the literature (14). The purity of arenobufagin, determined by high-performance liquid chromatography analysis, was more than 98% (Supplementary Figure S1, available at *Carcinogenesis* Online). Arenobufagin was dissolved in dimethylsulfoxide at a concentration of 500 μM and stored at −20°C.

Cell culture

Human HCC cell lines (HepG2, Hep3B and Bel-7402) and human breast adenocarcinoma cell line (MCF-7) were obtained from American Type Culture Collection (ATCC, Rockville, MD). Dox-resistant cancer cell lines HepG2/ADM (15) and MCF-7/ADR were kindly provided by Kwok-Pui Fung (School of Biomedical Sciences, The Chinese University of Hong Kong) and Li-Wu Fu (Cancer Center, Sun Yat-Sen University), respectively. All cell lines were incubated in RPMI-1640 (Invitrogen) supplemented with 10% (*v/v*) fetal bovine serum (Invitrogen) and 1% (*v/v*) penicillin–streptomycin (Invitrogen) at 37°C in a humidified atmosphere of 5% CO_2. Dox (1.2 μM) was added to the culture medium to maintain the multidrug-resistant characteristics of HepG2/ADM or MCF7/ADR cells.

3-(4,5-Dimethylthiazol-2-yl)-2,5-diphenyltetrazolium bromide assay

The growth inhibitory effect of arenobufagin in HepG2 and HepG2/ADM cells was detected by 3-(4,5-dimethylthiazol-2-yl)-2,5-diphenyltetrazolium bromide (MTT) assay as described previously (16).

Clonogenic survival assay

Cell proliferation ability was measured using colony formation assay. Approximately, 500 cells were seeded in each well of six-well plates. After 24 h, cells were treated with different concentrations of arenobufagin and incubated for another 24 h. Cells were then washed with phosphate-buffered saline (PBS) before being incubated in fresh medium and maintained in a humidified atmosphere of 5% CO_2 at 37°C for 10 days. Visible colonies were manually counted at four points of each well under an inverted phase-contrast IX51 microscope (Olympus).

Detection of apoptosis and mitochondrial membrane potential

Apoptosis was detected by Annexin V–FITC staining assay using Annexin V–FITC/PI apoptosis detection kit (Biouniquer Tech) according to the manufacturer's protocol. Arenobufagin-induced changes in mitochondrial membrane potential were measured using a lipophilic cationic fluorescent probe JC-1 as described previously (16).

Transmission electron microscope ultrastructural observation

After treatment with arenobufagin for 24 h, cells were fixed in ice-cold 4% glutaraldehyde in PBS (pH 7.4) at 4°C overnight. Cells were washed twice with PBS, post-fixed in 1% osmium tetroxide for 1 h, dehydrated in a graded series of ethanol and acetone and then embedded in Epon 618. Ultra-thin sections (0.1–0.5 μm) were cut, double-stained with uranyl acetate and lead citrate, then observed under a TECNAI-10 transmission electron microscope (Philips, Netherlands).

Cyto-ID staining assay

Cyto-ID is a proprietary reagent, which specifically labels autophagic vacuoles and co-localizes with light chain 3 (LC3). Cyto-ID® Autophagy detection kit (Enzo Life Sciences) was used according to the manufacturer's protocol. The fluorescence was measured by Tecan GeNios microplate reader (Tecan, Finland).

Monodansylcadaverine staining assay

Monodansylcadaverine (MDC), a lysosomotropic fluorescent compound, which selectively labels autophagic vacuoles, was used to assess autophagy induction by arenobufagin (17).

Immunofluorescence staining LC3

HepG2/ADM cells were fixed with methanol for 10 min at −10°C and washed three times with PBS. After blocking with 5% bovine serum albumin in PBS-T for 60 min, cells were incubated with anti-LC3B antibody (1:100) at 4°C overnight and then incubated with Alexa Fluor 488-conjugated antirabbit IgG antibody (1:100) in darkness for 60 min at room temperature. Samples were washed with PBS for three times and examined under confocal microscope (Carl Zeiss, Germany) with excitation and emission wavelengths of 488 and 520 nm, respectively.

Isolation of cytosol and mitochondrial fractions

The cytosol and mitochondrial fractions of HepG2 and HepG2/ADM cells were isolated and immunoblotted with antibody against Bax as described previously (18).

Western blot analysis

Preparation of total protein lysates and western blot analysis were performed as described previously (16).

Small interfering RNA transfection

HepG2 and HepG2/ADM cells were seeded in six-well plates and transfected at 60% confluency with siRNA duplexes against human Akt (100 nM), mTOR (100 nM), Beclin1 (60 nM), Atg5 (60 nM) or control siRNA by lipofectamine 2000 (Invitrogen) according to manufacturer's protocol. After 6 h incubation, the transfected cells were exposed to arenobufagin for various time points, followed by analysis of cell viability by MTT assay, of apoptosis by flow cytometry, or of autophagy by MDC staining assay. Transfection efficiency was determined to be more than 75% by fluorescein-labeled non-targeted siRNA control (Ambion).

Tumor xenograft in nude mice

Male *nu/nu* BALB/c mice (4–6 weeks old) were obtained from SJA Lab Animal (Hunan, China). The mice were fed with sterilized food and water and were housed in barrier environment with a light–dark cycle of 12 h:12 h. All animal research procedures conducted conformed to the guidelines for the care and use of laboratory animals published by the National Institutes of Health and were approved by the laboratory animals care and use committee of Jinan University. HepG2/ADM cells (1×10^7) were inoculated subcutaneously on the backs of nude mice and allowed to grow for ~7 days to reach a tumor volume of ~50 mm^3. Mice were randomly divided into three groups with six mice in each group. One of the groups was administered a daily intraperitoneal dose of 0.1% dimethylsulfoxide in PBS to serve as the vehicle control. The other two groups were administered daily with a low dosage of arenobufagin (3 mg/kg/day intraperitoneal) or high dosage of arenobufagin (6 mg/kg/day intraperitoneal). Feeding behavior and motor activity of the mice were carefully observed, and their body weights were measured every 3 days throughout the treatment period. Tumor volumes were measured every 3 days and calculated using the following formula: $a^2 \times b \times 0.4$, where a refers to the smaller diameter and b is the diameter perpendicular to a. The mice were killed at the end of the experiments. Tumor xenografts were removed and weighed. Part of each tumor tissue was stored at −80°C for western blot analysis.

Immunohistochemical and immunofluorescence staining analysis

Glutaraldehyde-fixed tumor specimens were embedded with paraffin and cut into 5 μm thin sections. Each tissue section was deparaffinized and underwent hematoxylin and eosin and immunofluorescence staining analysis, respectively. Immunofluorescence staining analysis was performed with anti-p-mTOR (Ser^{2448}) antibody (1:100) and Alexa Fluor 488-conjugated antirabbit IgG antibody (1:100), as mentioned previously.

Statistical analysis

All experiments were performed at least three times, and data were presented as mean ± standard error. GraphPad Prism 5.0 was used for statistical analysis. A difference was considered significant when $P < 0.05$.

Results

Arenobufagin inhibits growth of human tumor cells

The effect of arenobufagin on cell growth was investigated using MTT assay on several human cell lines. We first examined the effect of arenobufagin on the cell viability of human HCC cell lines (HepG2 and HepG2/ADM). As shown in Figure 1B, arenobufagin potently inhibited the growth of both HepG2 and HepG2/ADM cells in a dose- and time-dependent manner (Figure 1B, left panel), with IC_{50} values of 20.24 ± 3.84 nM and 7.46 ± 2.89 nM after 72 h treatment, respectively. Similarly, arenobufagin inhibited the growth of two other human hepatoma cell lines (Hep3B and Bel-7402), two human breast adenocarcinoma cell lines (MCF-7 and MCF-7/ADR) (Supplementary Table S2, available at *Carcinogenesis* Online) and other carcinoma cell lines (Supplementary Table S3, available at *Carcinogenesis* Online), implying a broad spectrum of the antitumor activity of arenobufagin. Of note, multidrug-resistant HepG2 cells (HepG2/ADM) and MCF-7/ADR were more sensitive to arenobufagin than its parent cells reflected by the results of cell viability assay. Colony formation

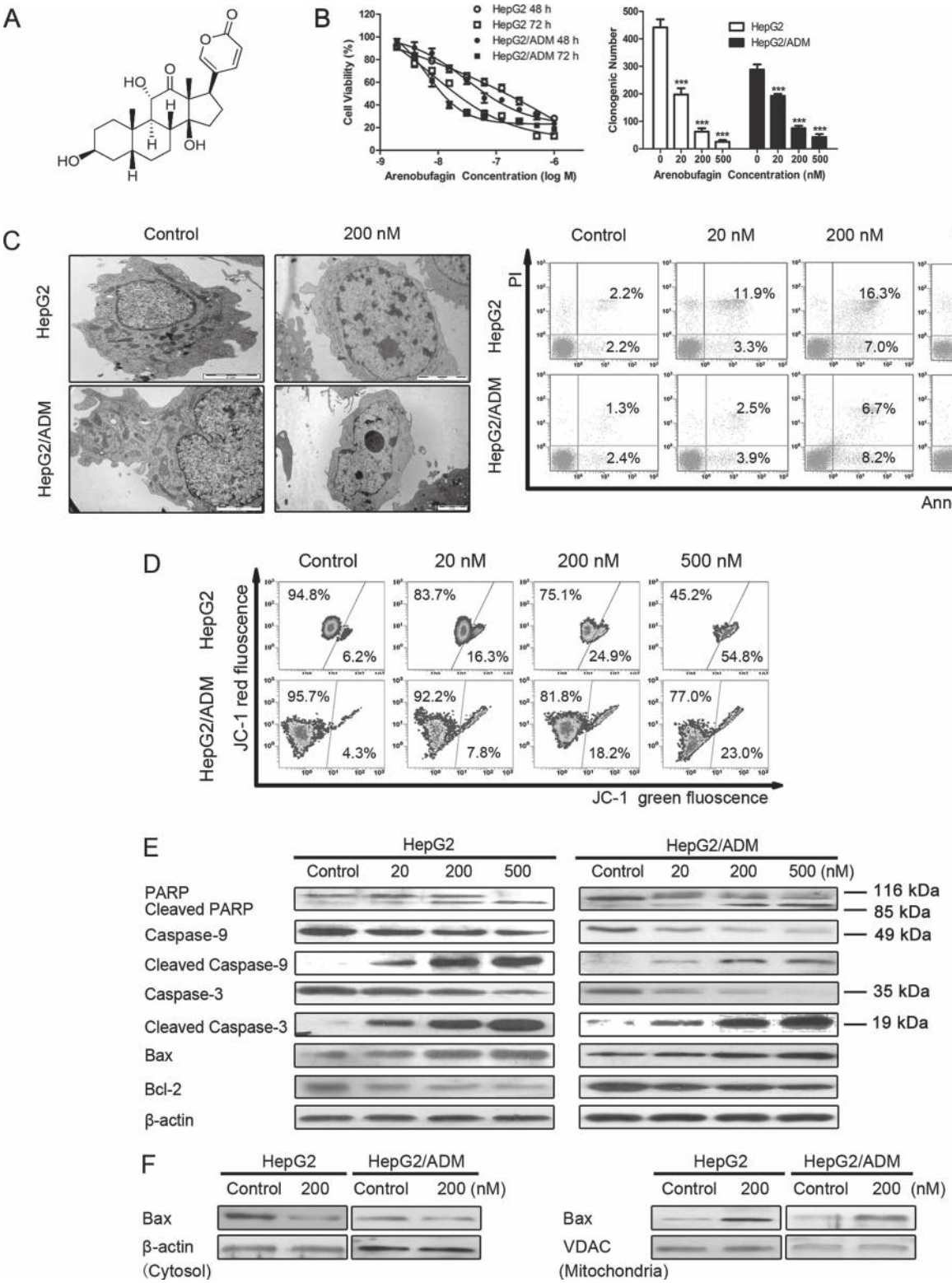

Fig. 1. Arenobufagin inhibits the proliferation of HCC cells and induces apoptosis *via* the mitochondrial pathways. (**A**) The chemical structure of arenobufagin. (**B**) Arenobufagin inhibits the proliferation of HepG2 and HepG2/ADM cells. The percentage of viable cells as measured by the MTT assay at 48 and 72 h relative to no-drug controls and arenobufagin concentrations were plotted as log-dose response curves (left panel). Clonogenic survival of hepatoma cells after arenobufagin treatment was measured by the number of clones capable of anchorage-dependent growth (right panel). (**C**) Arenobufagin induces apoptosis. Morphological changes of arenobufagin-treated cells as observed by TEM at 24 h. Original magnifications: 15 000×, 6200×; 15 000×, 6200×; Bar: 2, 5; 2, 2 μm (from left to right, left panel). Arenobufagin increases the percentage of annexin V-positive cells. After arenobufagin treatment for 24 h, the hepatoma carcinoma cells were stained with annexin V–FITC/PI and analyzed by flow cytometry (right panel). (**D**) Arenobufagin depolarizes mitochondrial membrane potential in hepatoma carcinoma cells. The hepatoma carcinoma cells were treated with or without arenobufagin for 24 h, then mitochondrial membrane potential was evaluated with flow cytometry after stained with fluorescent dye, JC-1. Distributions of red (JC-1 aggregates) versus green (JC-1 monomers) fluorescence in hepatoma cells were shown. (**E**) Effects of arenobufagin on expression of apoptosis-related proteins. Levels of PARP, caspase-9, caspase-3, Bax and Bcl-2 in total cell lysates from HepG2 and HepG2/ADM cells treated with arenobufagin at the indicated concentrations for 48 h were evaluated by western blot

assay further confirmed that arenobufagin inhibited the HCC cells proliferation in a dose-dependent manner (Figure 1B, right panel). HepG2 and HepG2/ADM cells were chosen to represent human HCC for the subsequent studies to elucidate the underlying molecular mechanisms of arenobufagin.

Arenobufagin induces apoptosis via mitochondrial apoptotic pathways

We found that arenobufagin induced apoptosis in HCC cells. Morphological changes in the ultrastructures of arenobufagin-treated cells were examined by transmission electron microscopy (TEM). Plasma membrane blebbing, shrinkage of nuclear membrane and chromatin condensation were observed in arenobufagin-treated HCC cells (Figure 1C, left panel), indicating the occurrence of apoptosis. Apoptotic cells were further quantified by Annexin V/PI doubling staining assay. Arenobufagin treatment increased the percentage of apoptotic (annexin positive) cells in HCC cells (Figure 1C, right panel and Supplementary Figure S2A, available at *Carcinogenesis* Online). By flow cytometry assay of JC-1-stained HCC cell lines, we discovered that arenobufagin led to depolarization of mitochondrial membrane in both HCC cell lines in a dose-dependent manner (Figure 1D), suggesting that arenobufagin triggered apoptosis *via* mitochondrial pathways. Western blot analysis revealed that specific cleavage of poly (ADP-ribose) polymerase (PARP) and a decrease in pro-caspase-9 and -3 were also induced by arenobufagin treatment (Figure 1E and Supplementary Figure S2B, available at *Carcinogenesis* Online). In addition, Bcl-2 level was decreased, whereas Bax level was increased (Figure 1E). Furthermore, a translocation of Bax from cytosol to mitochondria was also observed (Figure 1F). Taken together, arenobufagin induces apoptosis *via* the intrinsic mitochondrial pathways.

Arenobufagin causes autophagy in HepG2/ADM cells

Because HepG2/ADM cells showed lower sensitivity to arenobufagin-mediated apoptosis than HepG2 cells, we examined whether arenobufagin induced autophagy, which would have influenced the sensitivity of cancer cells to chemotherapy-induced apoptosis. After treatment with arenobufagin, autophagosomes and lysosomes were observed under TEM in some HepG2/ADM cells (Figure 2A), prompting that arenobufagin induced autophagic cell death, whereas simultaneously triggering apoptosis in other cells. Cyto-ID Green reagent staining showed the relative fluorescence intensity of cells was increased in a time-dependent manner, indicating the occurrence of autophagy (Figure 2B). Similar data are achieved through MDC staining (Figure 2C). Lipidation of microtubule-associated protein 1 LC3, as an autophagy marker, coats autophagosomes during autophagy and is converted to LC3-II resulting in the appearance of the delayed electrophoretic mobility in gel (19). LC3 immunofluorescence analysis showed punctuate LC3 II-labeled autophagolysosome vacuoles emitting green fluorescence were distinctly visible by fluorescence microscopy in the arenobufagin-treated HepG2/ADM cells as compared with control cells (Figure 2D). Treatment with arenobufagin (20 nM) at various time points led to a significant increase in LC3-II (Figure 2E). This increase could be further enhanced by the pretreatment of the cells with pepstatin A, a protease inhibitor, which inhibits LC3-II turnover (19) (Figure 2E). In addition, a trend of increased expression of other autophagy-associated proteins such as Beclin1, Atg5, Atg9 and Atg16L1 with attenuated expression of p62/SQSTM1 was also observed in arenobufagin treatment (Figure 2E). All these results supported the idea that arenobufagin induced autophagy in HepG2/ADM cells. Moreover, arenobufagin-induced autophagy was observed in HCC Hep3B, Bel-7402 and HepG2 cells as reflected by punctuate Cyto-ID and increased LC3-II (Supplementary Figure S3, available at *Carcinogenesis* Online).

Inhibition of autophagy enhances arenobufagin-induced apoptotic cell death

It has been reported that autophagy may facilitate cell survival in adverse microenvironment, and inhibition of autophagy may trigger increased induction of apoptosis in cells (20). Recent studies suggest that autophagy may cooperate with apoptosis to promote cell death (21,22). We, therefore, explored whether inhibition of autophagy increased apoptosis in HepG2/ADM cells under arenobufagin treatment. This transition to apoptosis can be interrogated using both pharmacological and genetic inhibitors of different points of the autophagic pathway and assessing the induction of apoptosis. Here, we use 3-methyladenine (3-MA), a specific autophagy inhibitor targeting the earliest stages of autophagosome formation, and chloroquine (CQ) and bafilomycin A (BA) that are autophagy–lysosomal inhibitors (23). Alternatively, inhibition of autophagy can be achieved by selective inhibition of Beclin1 and Atg5 using RNA interference. Beclin1 is an essential autophagic gene that contributes to the initial vesicle nucleation and formation of autophagosome, whereas Atg5 participates in autophagic vesicle elongation and completion. Both Beclin1 and Atg5 are common targets for autophagy inhibition. Pretreatment with 3-MA remarkably attenuated the formation of acidic autophagic vacuoles in the presence of arenobufagin (Figure 3A) and blocked the appearance of LC3-II in gel (Figure 3B). Addition of 3-MA also increased the sensitivity of HepG2/ADM cells toward the cytotoxic effect of arenobufagin (Figure 3C) and significantly increased the proportion of apoptotic cells as reflected by PARP cleavage and decreased caspase-9 and -3 when compared with those with arenobufagin alone (Figure 3B and D). Similar phenomena were observed in cells treated with the combinational exposure to arenobufagin and pharmacological inhibitors (CQ or BA1), as well as in cells after genetic knockdown of the essential autophagy genes Beclin1/Atg5 (Figure 3C and D). We also noticed that pretreatment with Beclin1/Atg5 siRNA duplexes could remarkably increase PARP cleavage in Hep3B and Bel-7402 cells treated with arenobufagin (Supplementary Figure S4, available at *Carcinogenesis* Online). In summary, these results suggested that autophagy may protect cells from arenobufagin-induced apoptotic cell death, and blocking autophagy by pharmacologic or molecular inhibition improves the killing effect of arenobufagin in HepG2/ADM cells through increased apoptosis.

Arenobufagin inhibits the activation of PI3K/Akt pathways

Given the critical role of PI3K/Akt pathway in controlling cell survival/death in response to external stimuli (24), we investigated if arenobufagin activates the PI3K/Akt pathway and if this pathway plays a central role in arenobufagin-mediated cell death. Western blot analysis showed that the levels of PI3 kinase P110α (the catalytic subunit of PI3K) and Akt (including the isoforms of Akt1, Akt2 and Akt3) were decreased in HCC cells treated with arenobufagin (Figure 4A, Supplementary Figures S5 and S6A, available at *Carcinogenesis* Online). Concomitantly, the degrees of phosphorylation of Akt at Ser^{473} and Thr^{308} and its upstream regulator PDK1 at Ser^{241} and downstream effector c-Raf at Ser^{259} were decreased, whereas phosphatase and tensin homologue deleted on chromosome ten (PTEN) phosphorylated at Ser^{380} increased (Figure 4A and Supplementary Figure S7A, available at *Carcinogenesis* Online). These data together imply that arenobufagin may inhibit Akt with involvement of PTEN activation as well as PDK1 and PI3K inhibition.

To further identify the role of Akt in arenobufagin-mediated cell growth inhibition, we employed the inhibitor LY294002 or Akt siRNA to silence Akt. We then examined the impact of arenobufagin on cell viability. The results showed that inactivation of Akt by LY294002 or silencing Akt by siRNA tremendously sensitized HCC cells toward cytotoxicity of arenobufagin (Figure 4B). Combinational treatment with arenobufagin and LY294002 or Akt siRNA also strikingly increased

←

analysis. β-actin was used as a loading control. (**F**) Effects of arenobufagin on translocation of Bax from cytosol to mitochondria. Level of Bax in cytosol and mitochondrial fractions from HepG2 and HepG2/ADM cells treated with arenobufagin at the indicated concentrations for 48 h were evaluated by western blot analysis. β-actin and Voltage-dependent anion channel (VDAC) were used as a loading control, respectively. ***$P \leq 0.001$, one-way analysis of variance (ANOVA), *post hoc* comparisons, Tukey's test. Columns, means; error bars, standard errors (SEs).

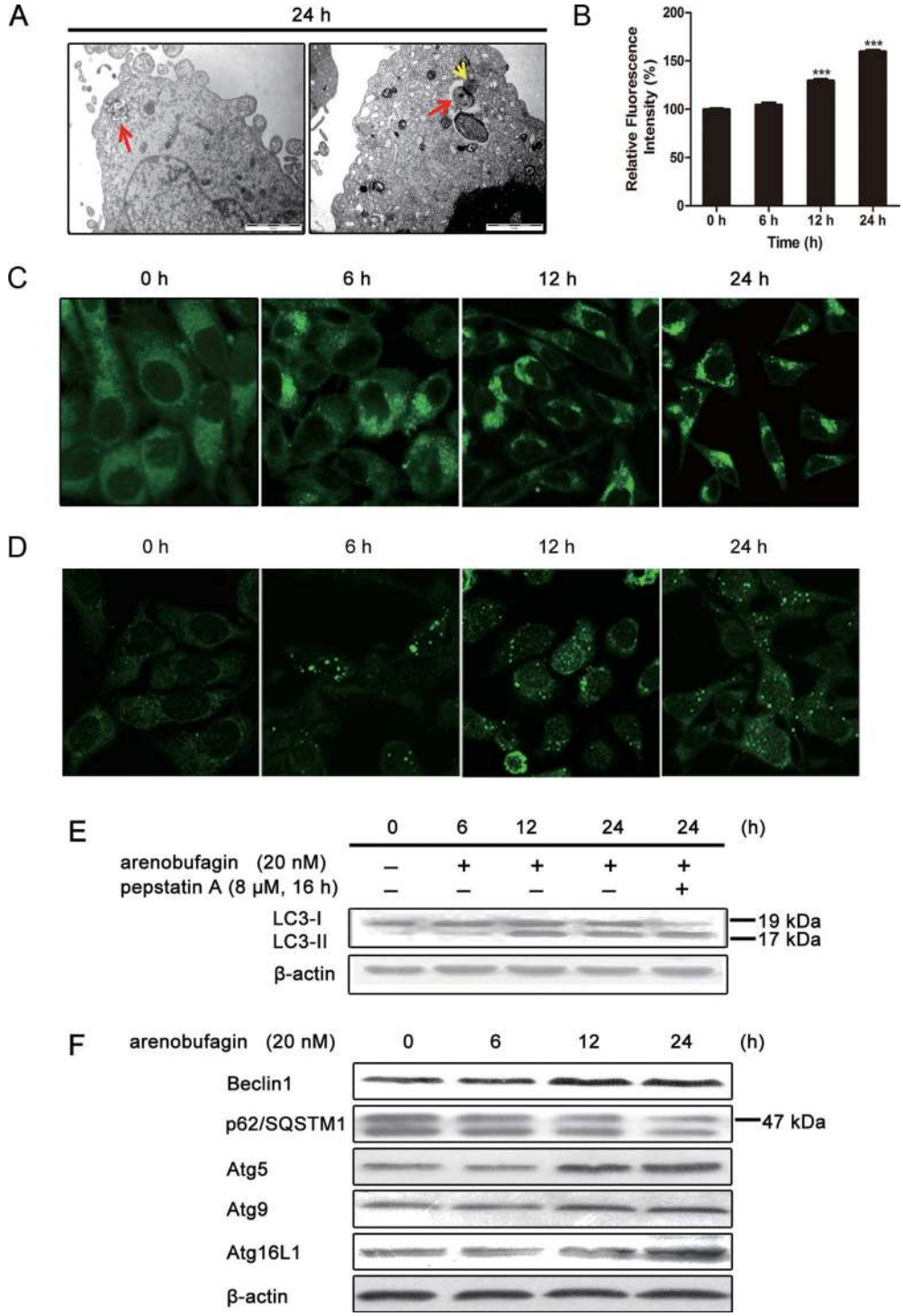

Fig. 2. Arenobufagin elicits autophagy in HepG2/ADM cells. (**A**) HepG2/ADM cells were treated with arenobufagin for 24 h, and ultrastructural changes were observed by TEM. Arrows indicate autophagosomes and arrow heads indicate lysosomes. Original magnification: 15 000×; Scale bar: 2 m. (**B**) Punctuate Cyto-ID-coated autophagosomes in arenobufagin-treated cells. HepG2/ADM cells were incubated with arenobufagin for 6, 12 and 24 h and stained with Cyto-ID for 30 min at 37°C. Intracellular Cyto-ID fluorescence was analyzed by Tecan GeNios microplate reader. (**C**) Punctuate MDC-coated autophagosomes in arenobufagin-treated cells. HepG2/ADM cells were incubated with arenobufagin for indicated time and stained with MDC (50 μM) for 15 min at 37°C. Intracellular MDC fluorescence was analyzed by confocal fluorescence microscopy. Original magnification: 640×. (**D**) LC3 location and expression after arenobufagin treatment. LC3 immunofluorescence in HepG2/ADM cells after arenobufagin treatment. Cells were treated with arenobufagin (20 nM) for 6, 12 and 24 h and incubated with anti-LC3 antibody and Alexa Fluor 488-conjugated antirabbit IgG antibody. Cells were observed by confocal fluorescence microscopy. Original magnification: 640×. (**E**) Immunoblot analysis of LC3 in HepG2/ADM treated by arenobufagin. (**F**) Effects of arenobufagin on expression of autophagy regulatory proteins. ***$P \leq 0.001$, one-way ANOVA, *post hoc* comparisons, Tukey's test. Columns, means; error bars, SEs.

apoptosis as detected by PARP cleavage and decrease of caspase-9 and -3 (Figure 4C and D and Supplementary Figure S6B, available at *Carcinogenesis* Online). Moreover, pretreatment with PI3K activator (50 μg/ml) attenuated arenobufagin-induced apoptosis in HepG2/ADM cells (Figure 4E, top panel). These results together revealed the inhibition of activation of PI3K/Akt pathway by arenobufagin and its central

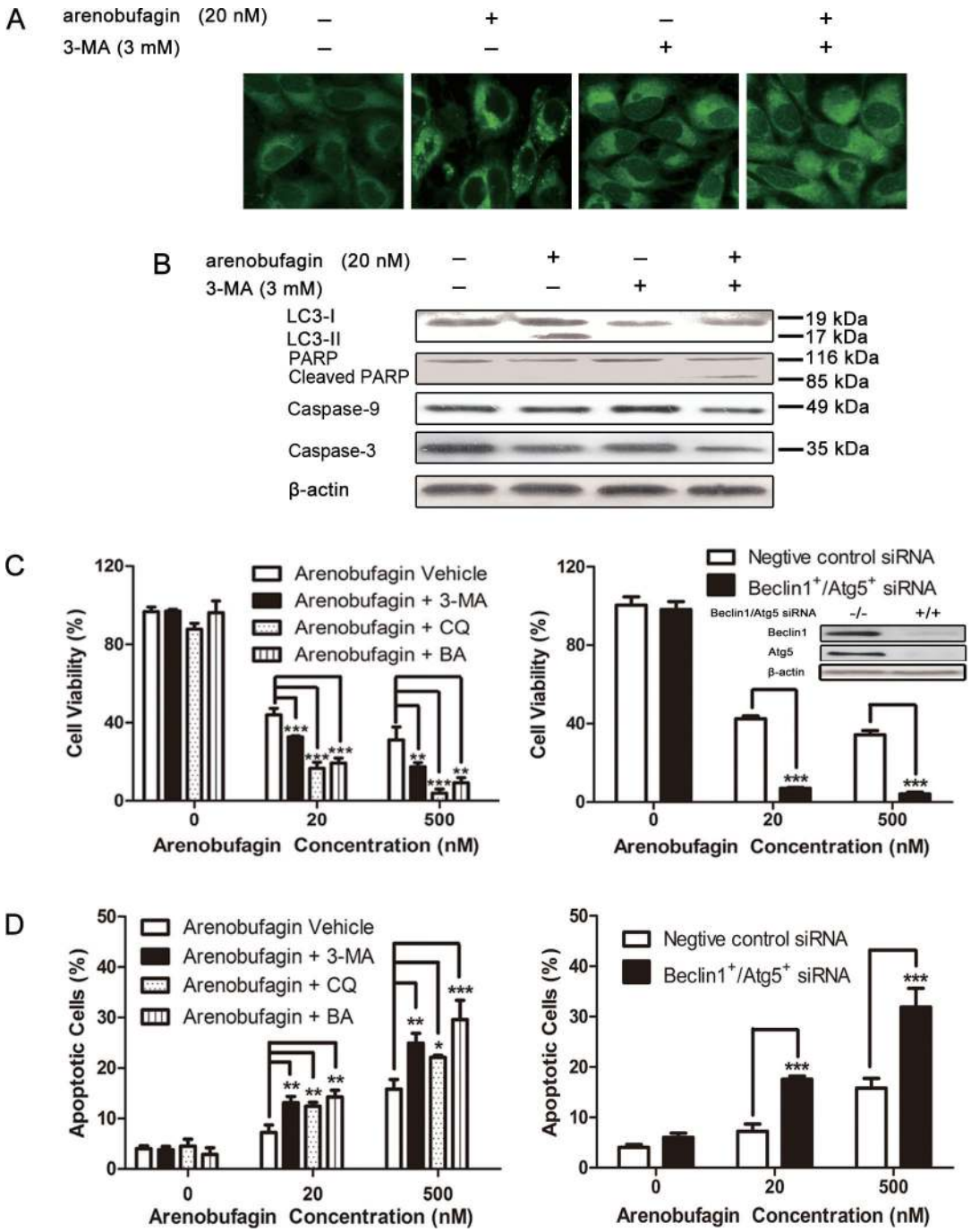

Fig. 3. Inhibition of autophagy enhances apoptosis in arenobufagin-treated HepG2/ADM cells. Cells were pretreated with 3-MA (3 mM) for 30 min prior to a 24 h treatment with arenobufagin. (**A**) 3-MA effectively inhibits the formation of autophagic vacuoles. Original magnification: 640×. (**B**) Inhibition of autophagy by 3-MA enhances PARP cleavage and decreases caspase-9 and -3 in arenobufagin-treated HepG2/ADM cells. (**C**–**D**) HepG2/ADM cells treated with the combination of arenobufagin and 3-MA, CQ (20 μM), BA (10 nM) (left panel) or Beclin^{+}/Atg5^{+} siRNA duplexes (each, right panel). Cell viability was assayed (**C**) or annexin V-positive cells were quantitatively analyzed (**D**). $^{*}P \le 0.05$, $^{**}P \le 0.01$, $^{***}P \le 0.001$, one-way ANOVA, *post hoc* comparisons, Tukey's test. Columns, means; error bars, SEs.

role in regulating apoptosis mediated by arenobufagin. Besides, arenobufagin-induced autophagy was slightly decreased in HepG2/ADM cells in the presence of PI3K activator (Figure 4E, bottom panel).

Dual role of mTOR in arenobufagin-induced apoptosis and autophagy

We further explored the impact of arenobufagin on mTOR, an important downstream executor of Akt. Arenobufagin treatment led to a marked decrease in mTOR and phosphorylated mTOR Ser^{2448} and Ser^{2881} (Figure 5A and Supplementary Figure S7A, available at *Carcinogenesis* Online). mTOR can bind to Raptor to form rapamycin-sensitive TORC1 complex, which controls phosphorylation of p70S6K (70 kDa ribosomal S6 kinase (24)), also mTOR binds with another partner, Rictor, to form a rapamycin-insensitive complex, TORC2, which in turn modulates Ser^{473} phosphorylation of Akt (25). We, therefore, examined the effect of arenobufagin on these proteins. Arenobufagin decreased the levels of Raptor and p70S6K phosphorylated at Thr^{389} (Figure 5A). In contrast with the elements in the TORC1 complex, Rictor expression was unchanged after arenobufagin treatment (Figure 5A), indicating that the PI3K/Akt pathway

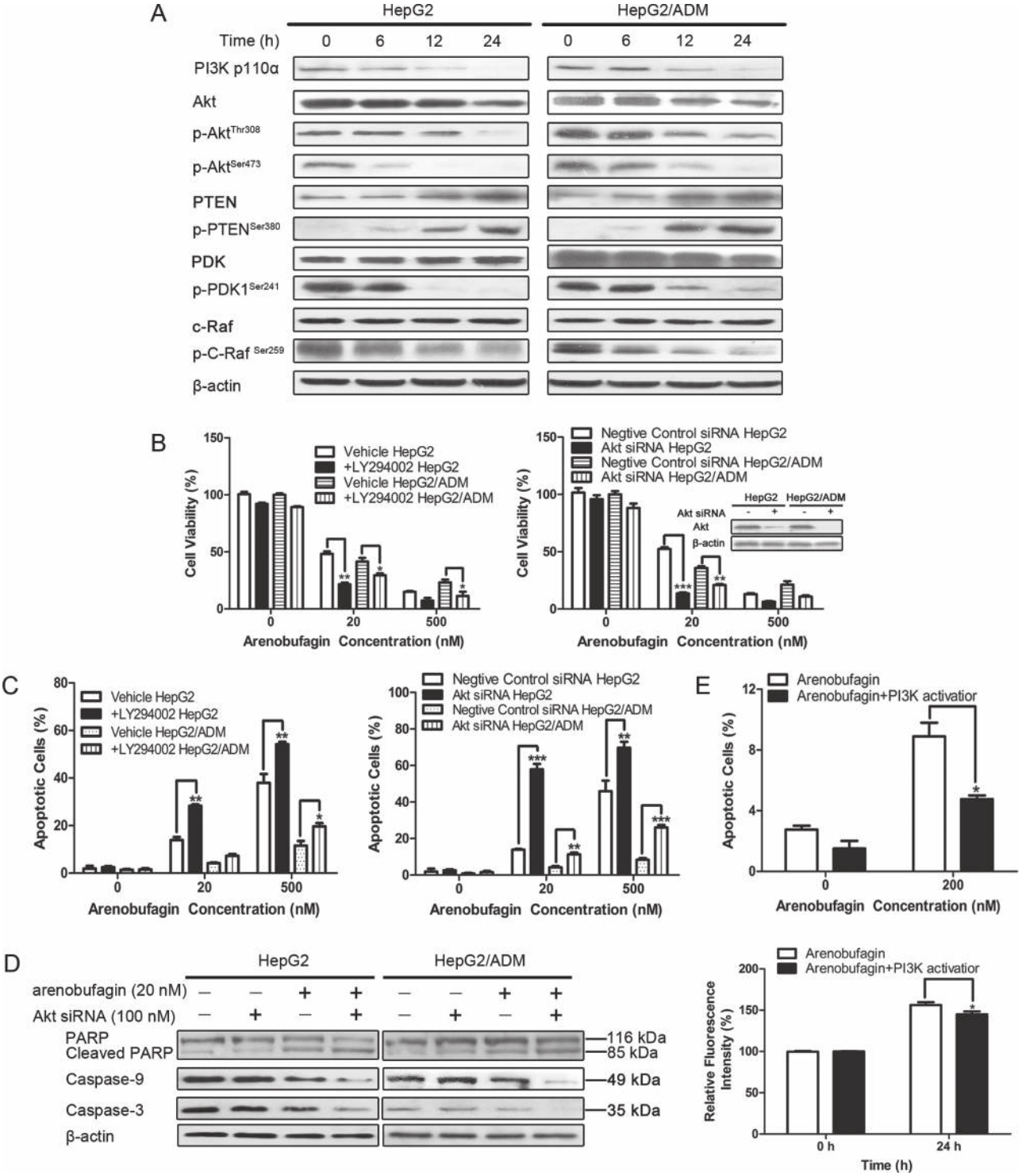

Fig. 4. Arenobufagin inhibits the aberrant activation of PI3K/Akt pathway. (**A**) Arenobufagin inhibits Akt signaling with increased PTEN. HepG2 and HepG2/ADM cells were treated with arenobufagin, and expressions of Akt, p-Akt^{Thr308}, p-Akt^{Ser473}, PTEN, p-PTEN^{Ser380}, PDK1, p-PDK1^{Ser241}, c-Raf and p-c-Raf^{Ser259} in total cell lysates were evaluated by western blot analysis. (**B**–**D**) HepG2/ADM cells were treated with arenobufagin in the absence or presence of LY294002 (4 μM) and Akt siRNA (100 nM). Cell viability was measured by MTT assay (B), and the proportion of annexin V-positive cells was analyzed by flow cytometry (C) or by immunoblotting with anti-PARP, anticaspase-9 and anticaspase-3 (D). (**E**) Effect of PI3K activator on arenobufagin-induced apoptosis (top panel) and autophagy (bottom panel). HepG2/ADM cells were treated with arenobufagin in the absence or presence of PI3K activator (50 μg/ml) for 24 h. The proportion of annexin V-positive apoptotic cells was analyzed by flow cytometry. For detection of autophagy level, cells were stained with Cyto-ID for 30 min at 37°C and intracellular Cyto-ID fluorescence was analyzed by Tecan GeNios microplate reader. *$P \le 0.05$, **$P \le 0.01$, ***$P \le 0.001$, one-way ANOVA, *post hoc* comparisons, Tukey's test. Columns, means; error bars, SEs.

may not be regulated by the Rictor–mTOR complex in arenobufagin-treated HCC cells.

As mTOR is a well-known regulator of autophagy, the involvement of mTOR in the progress of autophagy in arenobufagin-treated cells was further consolidated. Fluorescence microscopy shows significant increase in the number of MDC-labeled vacuoles (Figure 5B) and western blotting analysis reveals higher LC3-II expression (Figure 5D) in cells treated with both mTOR blockers and arenobufagin compared

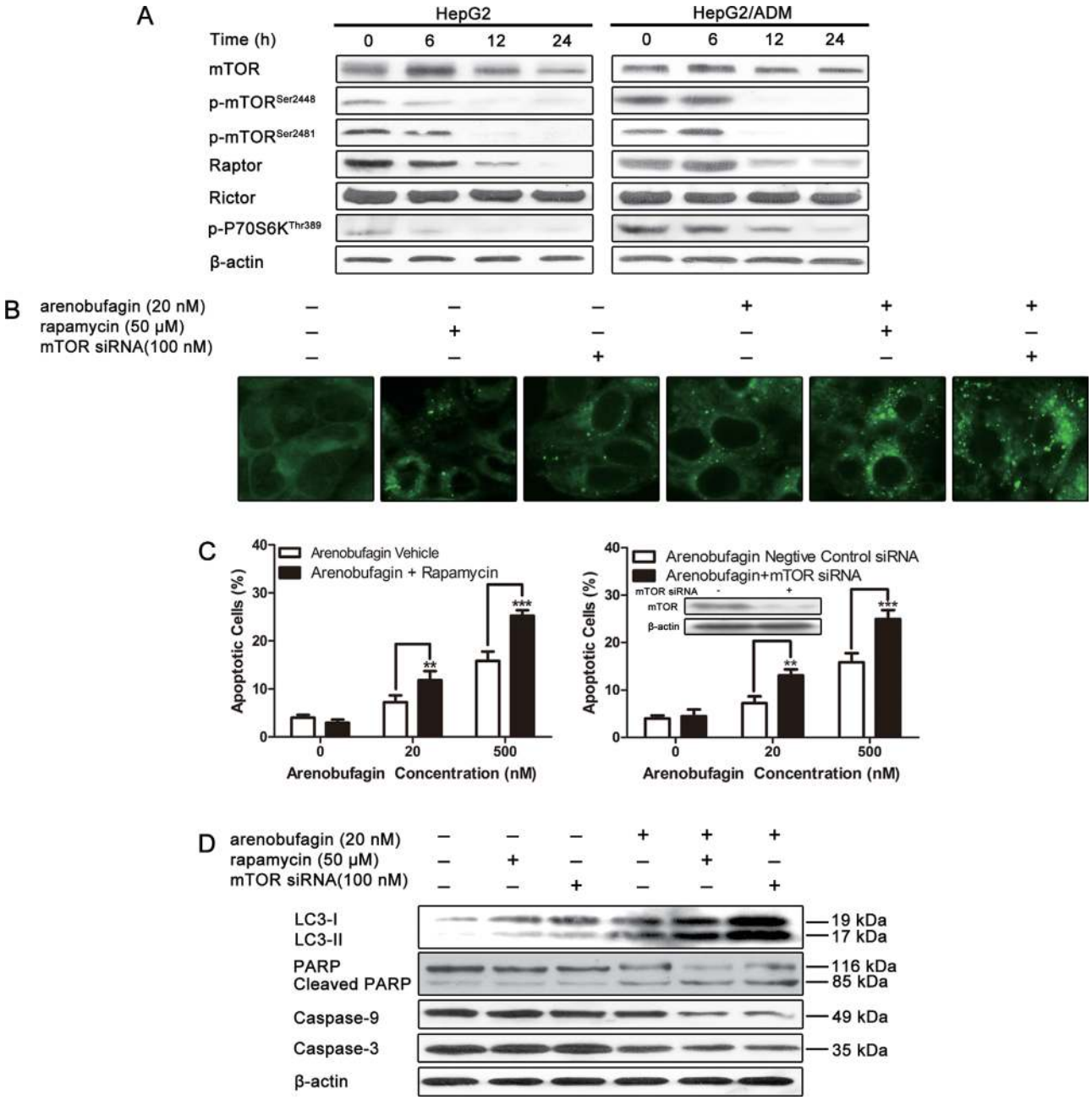

Fig. 5. The role of mTOR in arenobufagin-induced apoptosis and autophagy. (**A**) Arenobufagin inhibits mTOR signaling. HepG2 and HepG2/ADM cells treated with arenobufagin, and levels of mTOR, p-mTOR^{Ser2448}, p-mTOR^{Ser2481}, p-P70S6K^{Ser389}, Raptor and Rictor in total lysate were evaluated by western blot analysis. (**B**) MDC-labeled vacuoles in HepG2/ADM cells treated with rapamycin (50 μM) for 30 min or transfected with mTOR siRNA (100 nM) for 6 h prior to 12 h treatment with arenobufagin. Original magnification: 640×. (**C**) Apoptosis induction by arenobufagin in HepG2/ADM cells pretreated with rapamycin (left panel) or transfected with siRNA targeting mTOR (right panel). The proportion of apoptotic cells was measured by flow cytometry. (**D**) Effects of arenobufagin with rapamycin or mTOR siRNA on proteins associated with autophagy and apoptosis. Levels of LC3, PARP, caspase-9 and caspase-3 in total cell lysates from HepG2/ADM cells were evaluated by western blot analysis. $^{**}P \leq 0.01$, $^{***}P \leq 0.001$, one-way ANOVA, *post hoc* comparisons, Tukey's test. Columns, means; error bars, SEs.

with arenobufagin treatment alone. Taken together, this is evidence of increased autophagy. In addition, combined treatment of mTOR blockers and arenobufagin strikingly increased the population of annexin V-positive cells (Figure 5C) as well as specific cleavage of PARP, caspase-9 and -3 (Figure 5D) compared with arenobufagin treatment alone. This data indicate the induction of apoptosis. As expected, silencing mTOR with siRNA also significantly enhanced autophagy and apoptosis with arenobufagin treatment (Figure 5B–D and Supplementary Figure S7B, available at *Carcinogenesis* Online). These data suggest that mTOR is involved in the regulation of both autophagy and apoptosis induced by arenobufagin. Inhibition of mTOR promoted the development of both autophagy and apoptosis.

Arenobufagin inhibits growth of HepG2/ADM cells xenografts in nude mice

In vivo anti-HCC activity of arenobufagin was evaluated in HepG2/ADM xenografts in nude mice. After administration of arenobufagin at 3 and 6 mg/kg/day in mice with HepG2/ADM xenografts for 28 d, the tumor volume was significantly reduced by 42% and 51%, respectively (Figure 6A and B) compared with placebo controls. The

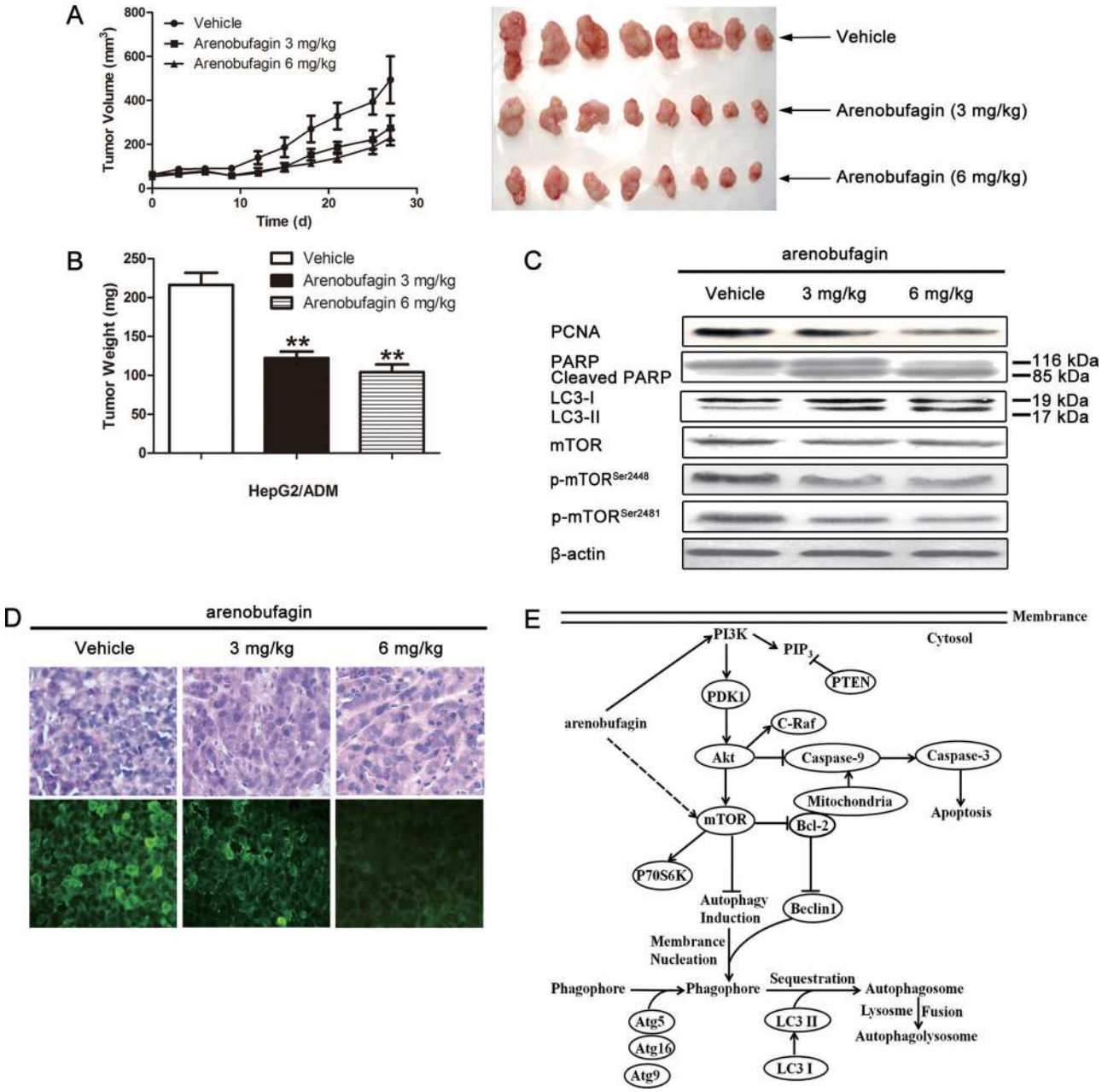

Fig. 6. *In vivo* antitumor efficacy of arenobufagin. (**A**) Inhibition of the growth of HepG2/ADM xenograft tumors by arenobufagin. BALB/c nude mice bearing HepG2/ADM xenograft tumors were treated with either a vehicle (0.1% dimethylsulfoxide solvent control) or arenobufagin (3 or 6 mg/kg/day) from day 7 to day 34 after inoculation of HepG2/ADM cells. The growth curves of subcutaneous xenografts of HepG2/ADM were shown (left panel). Representative tumors removed were photographed (right panel). (**B**) The tumor weights of mice after arenobufagin treatment. (**C**) Proliferating cell nuclear antigen, PARP, LC3 as well as the total and phosphorylated mTOR in tumor tissue lysates from vehicle- and arenobufagin-treated mice were detected by western blot analysis. (**D**) Arenobufagin downregulates phosphorylation of mTOR detected with fluorescent immunostaining by using anti-p-mTOR^{Ser2448}. Original magnification: 20×. Hematoxylin and eosin staining (upper panel) and immunofluorescence analysis of mTOR expression *in vivo* (lower panel). (**E**) A proposed model of web interaction to delineate the actions of arenobufagin. ⊥ indicates an inhibitory effect. $^{**}P \leq 0.01$, one-way ANOVA, *post hoc* comparisons, Tukey's test. Columns, means; bars, SEs.

size and weight of tumors were obviously lower in treated groups than in control group (Figure 6B). Mice in the arenobufagin group maintained normal weight gain throughout treatment (Supplementary Figure S8, available at *Carcinogenesis* Online) and did not show any abnormality in food intake or behavior. Western blot analysis in tissues from xenografts showed remarkable decrease in levels of proliferating cell nuclear antigen, PARP, total and phosphorylated mTOR as well as increase of LC3-II in arenobufagin-treated mice compared with control group (Figure 6C). Immunostaining of histological sections for mTOR also showed that arenobufagin decreased the degree of phosphorylation of mTOR at Ser^{2448} (Figure 6D). These *in vivo* data suggested that arenobufagin inhibits tumor growth and induces apoptosis and autophagy with suppression of mTOR in HCC cells.

Discussion

Arenobufagin, one of components of toad venom, which is listed in Chinese Pharmacopoeia and used to treat liver cancer in TCM, was only reported to be an effective cardiotonic agent (11). As arenobufagin showed the most potent anti-HCC activity among all isolated cytotoxic bufadienolides (such as bufalin, arenobufagin, cinobufagin, telocinobufagin and hellebrigenin) (9,10) and had high content

in toad venom (about 1.75%) (26), we speculated that arenobufagin may be one of the central active ingredients of toad venom for the treatment of liver cancer. In this study, we demonstrated that arenobufagin markedly inhibited the proliferation of a wide variety of tumor cells including HCC cells. Arenobufagin was effective against not only Hep3B cells with HBV infection but also drug-sensitive HepG2 cells as well as multidrug-resistant HepG2/ADM cells. Its anti-HCC activity *in vivo* without weight loss or any other life-threatening toxicities in animals supports its potential for further clinical investigation for liver cancer treatment. To our knowledge, this is the first report of the antineoplastic activity of arenobufagin against HCC.

Our data showed that arenobufagin induces mitochondria-mediated apoptosis in HepG2 and HepG2/ADM cells, accompanied by a decrease of mitochondrial potential, increase of Bax/Bcl-2 expression ratio and Bax translocation from cytosol to mitochondria, activation of caspase-3 and -9 as well as cleavage of PARP. In accord with our findings, some researchers reported that bufalin, a representative bufadienolide, inhibits the growth of a wide variety of cancer cells through induction of apoptosis and differentiation (27–29), which is dependent on the molecular mechanisms involving downregulation of vascular endothelial growth factor receptor 1/2 (30), activation of Ap-1 *via* the Ras/Raf/mitogen-activated protein kinase cascade (31,32), regulation of protein kinase C isozymes (33), inhibition of Na^+, K^+-adenosine triphosphatase (34) and initiation of Fas- and mitochondria-mediated apoptosis pathways (35).

It is intriguing that the apoptotic rate in HepG2/ADM cells was much lower than that of HepG2 cells suggesting the presence of a cytoprotective mechanism. We thus examined whether arenobufagin induced autophagy. Autophagy is a catabolic process in which cells respond to various stress stimuli, such as hypoxia, nutrient starvation and DNA damage (36). In this process, proteins or organelles, sequestered by double-membrane structures, fuse with lysosomes and are subsequently degraded by lysosomal hydrolases to be recycled to sustain metabolism (37). However, the exact role of autophagy in cancer treatment, and whether it protects cells from cytotoxic effects of anticancer drugs by blocking apoptosis or kills cells as an alternate pathway of cell death is still controversial (38,39). Our data revealed that arenobufagin could induce autophagy accompanied by apoptosis in HepG2/ADM cells. We found that inhibition of autophagy by specific inhibitors (3-MA, BA and CQ) or $Beclin1^+$/$Atg5^+$ siRNA markedly decreased cell viability and significantly increased apoptosis. Collectively, these results indicate that autophagy provides a protective mechanism against arenobufagin-induced apoptosis.

Increasing evidence indicates that the cross talk between autophagy and apoptosis is made especially complicated by the fact that they share many common regulatory molecules, such as p53, Bcl-2 and the PI3K/Akt/mTOR signaling pathway (40,41). It is well known that the PI3K/Akt/mTOR pathway plays an important role in cell growth, survival, differentiation and metabolism (24). Inhibition of PI3K/Akt/mTOR signaling pathway causes cell death associated with apoptosis and/or autophagy (42,43). The present results indicate that arenobufagin regulates Akt and mTOR, as well as other key molecules PTEN, PDK1, c-Raf and p70S6K in PI3K/Akt/mTOR pathway. Either Akt-specific inhibitor LY294002 or Akt gene silencing by siRNA pretreatment caused the decrease in cell viability and corresponding increase of apoptosis, in comparison with arenobufagin treatment alone. It has been reported that phosphorylation of Akt at Thr^{308} can regulate protein synthesis, proliferation and cell shape, whereas phosphorylation of Akt at Ser^{473} is associated with resistance to apoptosis by controlling subcellular localization of pro-apoptotic proteins (24). Our data showed that the decrease in Akt^{Ser473} phosphorylation in HepG2 cells was more and happened earlier than that of HepG2/ADM cells at the same concentration, whereas the decrease in Akt^{Ser308} phosphorylation was not obviously different in both cell lines. Considered that the apoptotic rate was higher in HepG2 cells, it can be concluded that phosphorylation of Akt at Ser^{473} may play a protective role in arenobufagin-induced apoptosis. Furthermore, mTOR inhibitor rapamycin or mTOR siRNA pretreatment not only enhances the apoptotic-inducing activity and anticancer efficacy of arenobufagin but also potentiates autophagy induction. Consistently, PI3K activator pretreatment decreased the appearance of apoptosis and autophagy induced by arenobufagin, which further proved the critical role of PI3K/Akt/mTOR pathway. The phenomenon in which inhibition of mTOR enhances arenobufagin-induced autophagy is consistent with the notion that inhibiting the PI3K/Akt/mTOR pathway stimulates autophagy, namely, mTOR regulates various steps of autophagosomal vesicle formation by the functions downstream Atg1 Ser/Thr protein kinase complex or stimulates autophagocytosis by activating p70S6K *via* a feedback inhibition of insulin signaling pathway to activate the FoxO3 pathway (40). It should also be pointed out that mTOR has broad functions other than autophagy induction. Previous studies also have proven mTOR to be a regulator of apoptosis in various cancer cells (44–46). It was recently reported that mTOR inhibitor rapamycin could downregulate Bcl-XL to promote apoptosis (47). Moreover, the downstream target of mTOR, p70S6K, can potently block Bad-induced apoptosis by phosphorylation of Bad at S136 site to disrupt Bad's binding to Bcl-XL and/or Bcl-2 (48). Thus, inhibition of mTOR possibly increases apoptosis. Given that autophagy may antagonize apoptosis in arenobufagin-treated cells, it seems to be controversial that stimulation of autophagy and apoptosis appears simultaneously after rapamycin or mTOR siRNA pretreatment. However, it should be taken into account that there are three types of autophagy: (i) basal housekeeping autophagy, which is important for protein and organelle turnover; (ii) starvation and DNA damage-induced autophagy, which promotes cell survival and (iii) autophagy that exceeds the safe threshold and leads to cell death (38). Scott *et al.* (49) found that cells with high levels of Atg1-induced autophagy are rapidly eliminated by hardwiring of the autophagic process to pro-apoptotic signals. Therefore, it is speculated that inhibition of mTOR by rapamycin or mTOR siRNA pretreatment not only induces apoptosis but also markedly enhances the autophagy and the excessive autophagy may act as apoptosis partners to induce cell death. Our results first demonstrated that mTOR might act as an important factor governing the cross talk between apoptosis and autophagy. Nevertheless, the role of mTOR in modulating arenobufagin-induced cell death appears complicated and needs to be further explored.

It has recently been demonstrated that the aberrant activation of PI3K/Akt/mTOR signaling pathway is implicated to a poor prognosis and has a critical role in the pathogenesis of HCC. The inhibition of this pathway decreases the lipogenesis activation and hepatocarcinogenesis as well as benign prognosis of human HCC. mTOR inhibitors such as everolimus and sirolimus show antineoplastic effects in human HCC (50,51). In this study, we noticed arenobufagin could induce apoptosis and autophagy on several HCC cells, suggesting that the compound has comprehensive effects on HCC cells. Moreover, the appearance of apoptosis and autophagy after arenobufagin treatment is closely linked to the inhibition of PI3K/Akt/mTOR pathway, demonstrating this pathway plays a pivotal role in HCC treatment. Besides, given that arenobufagin-induced apoptosis and autophagy, which protected cells from apoptotic cell death were both enhanced after the inhibition of mTOR, it should be pointed out that this pathway has a controversial role in HCC treatment. It seems necessary to combine chemotherapeutics with autophagy inhibitors for liver cancer treatment in some specific conditions. We also noticed that some proteins associated with PI3K pathway were changed after arenobufagin treatment. It might be due to that arenobufagin affects the upstream of PI3K/Akt/mTOR pathway (such as Na^+/K^+-adenosine triphosphatase) or the effects of arenobufagin are multiple targets. However, it is no doubt that the antineoplastic mechanisms of arenobufagin are complex. The research on targets and molecular mechanisms underlying many changed proteins is undergoing at present.

In summary, we demonstrated the cell growth inhibitory effect of arenobufagin from toad venom on HCC cells both *in vitro* and *in vivo*. We elucidated the underlying mechanism that involves cross talk between apoptosis and autophagy *via* inhibition of PI3K/Akt/mTOR

pathway (Figure 6E). Our study provides a rationale for the application of arenobufagin to be a potent chemotherapeutic agent for the treatment of liver cancer.

Supplementary material

Supplementary Figures S1–S8 and Tables S1–S3 can be found at http://carcin.oxfordjournals.org/

Funding

National Science Foundation of China (90913020, 30901847, 81025021 and 90713036); Science and Technology Program of China (2012ZX09103101-053) and Guangzhou City (2011J2200045 and 2011Y1-00017); Changjiang Scholars and Innovative Research Team in University (IRT0965) and the 973 Program grant (2009CB825506).

Acknowledgements

Special thanks to Dr Kurt Degenhardt (Touro College of Osteopathic Medicine, New York) for his comments on the manuscript. Special thanks to Mr Yunfeng Shi and Ms Hailan Tang (Test and Analysis Center, Jinan University, China) for their kind assistance in cell morphology observation by TEM and confocal microscopy. Sincere thanks to Mr Haifeng Yang (Guangdong Provincial TCM Hospital, China) for his help in preparation and observation of hematoxylin and eosin-stained histological sections. Thanks for Dr Jianxin Pang (Southern Medical University, China) for his guidance in tumor xenograft of nude mice.

Conflict of Interest Statement: None declared.

References

1. Jemal,A. *et al.* (2011) Global cancer statistics. *CA. Cancer J. Clin*., **61**, 69–90.
2. McGlynn,K.A. *et al.* (2005) Epidemiology and natural history of hepatocellular carcinoma. *Best Pract. Res. Clin. Gastroenterol*., **19**, 3–23.
3. Vitale,A. *et al.* (2010) Use of sorafenib in patients with hepatocellular carcinoma before liver transplantation: a cost-benefit analysis while awaiting data on sorafenib safety. *Hepatology*, **51**, 165–173.
4. Siegel,R. *et al.* (2011) Cancer statistics, 2011: the impact of eliminating socioeconomic and racial disparities on premature cancer deaths. *CA. Cancer J. Clin*., **61**, 212–236.
5. Tang,J. *et al.* (2008) Research progress on clinical application of venenum bufonis preparatian as antineoplastic drug. *China Pharmaceuticals,* **17**, 15–16.
6. Liu,J.S. *et al.* (2009) Antitumor effects of toad venom and its active components. *J. Int. Pharm. Res.,* **4**, 115–120.
7. Kamano,Y. *et al.* (2002) QSAR evaluation of the Ch'an Su and related bufadienolides against the colchicine-resistant primary liver carcinoma cell line PLC/PRF/5(1). *J. Med. Chem*., **45**, 5440–5447.
8. Hu,Y. *et al.* (2011) Comprehensive chemical analysis of Toad venom by using liquid chromatography/electrospray ionization tandem mass spectrometry. *J. Pharm. Biomed. Anal*., **56**, 210–220.
9. Tian,H.Y. *et al.* (2010) Bufogargarizins A and B: two novel 19-norbufadienolides with unprecedented skeletons from the venom of Bufo bufo gargarizans. *Chemistry*, **16**, 10989–10993.
10. Tian,H.Y. *et al.* (2010) New bufadienolides and C(23) steroids from the venom of Bufo bufo gargarizans. *Steroids*, **75**, 884–890.
11. Cruz,J.S. *et al.* (1993) Arenobufagin, a compound in toad venom, blocks Na(+)-K+ pump current in cardiac myocytes. *Eur. J. Pharmacol.*, **239**, 223–226.
12. Cruz,J.S. *et al.* (1994) Depressive effects of arenobufagin on the delayed rectifier K+ current of guinea-pig cardiac myocytes. *Eur. J. Pharmacol.*, **266**, 317–325
13. Li,M. *et al.* (2012) Arenobufagin, a bufadienolide compound from toad venom, inhibits VEGF-mediated angiogenesis through suppression of VEGFR-2 signaling pathway. *Biochem. Pharmacol*., **83**, 1251–1260.
14. Hofer,P. *et al.* (1960) Toad poisons. 22. Isolation of arenobufagin and other unknown bufogenins from Ch'an Su. *Helv. Chim. Acta.,* **43**, 1950.
15. Chan,J.Y. *et al.* (2000) Inhibition of P-glycoprotein expression and reversal of drug resistance of human hepatoma HepG2 cells by multidrug resistance gene (mdr1) antisense RNA. *Life Sci*., **67**, 2117–2124.
16. Zhang,D.M. *et al.* (2012) Bufotalin from Venenum Bufonis inhibits growth of multidrug resistant HepG2 cells through G2/M cell cycle arrest and apoptosis. *Eur. J. Pharmacol*., **692**, 19–28.
17. Gao,M. *et al.* (2008) OSU-03012, a novel celecoxib derivative, induces reactive oxygen species-related autophagy in hepatocellular carcinoma. *Cancer Res*., **68**, 9348–9357.
18. Kim,W.H. *et al.* (2004) Critical role of reactive oxygen species and mitochondrial membrane potential in Korean mistletoe lectin-induced apoptosis in human hepatocarcinoma cells. *Mol. Pharmacol*., **66**, 1383–1396.
19. Klionsky,D.J. *et al.* (2008) Guidelines for the use and interpretation of assays for monitoring autophagy in higher eukaryotes. *Autophagy*, **4**, 151–175.
20. Xu,Z.X. *et al.* (2007) A plant triterpenoid, avicin D, induces autophagy by activation of AMP-activated protein kinase. *Cell Death Differ*., **14**, 1948–1957.
21. Dalby,K.N. *et al.* (2010) Targeting the prodeath and prosurvival functions of autophagy as novel therapeutic strategies in cancer. *Autophagy*, **6**, 322–329.
22. Bareford,M.D. *et al.* (2011) Sorafenib enhances pemetrexed cytotoxicity through an autophagy-dependent mechanism in cancer cells. *Autophagy*, **7**, 1261–1262.
23. O'Donovan,T.R. *et al.* (2011) Induction of autophagy by drug-resistant esophageal cancer cells promotes their survival and recovery following treatment with chemotherapeutics. *Autophagy*, **7**, 509–524.
24. Hennessy,B.T. *et al.* (2005) Exploiting the PI3K/AKT pathway for cancer drug discovery. *Nat. Rev. Drug Discov*., **4**, 988–1004.
25. Ciuffreda,L. *et al.* (2010) The mTOR pathway: a new target in cancer therapy. *Curr. Cancer Drug Targets*, **10**, 484–495.
26. Zhang,P. *et al.* (2005) Quality evaluation of traditional Chinese drug toad venom from different origins through a simultaneous determination of bufogenins and indole alkaloids by HPLC. *Chem. Pharm. Bull*., **53**, 1582–1586.
27. Zhang,L. *et al.* (1992) Induction by bufalin of differentiation of human leukemia cells HL60, U937, and ML1 toward macrophage/monocyte-like cells and its potent synergistic effect on the differentiation of human leukemia cells in combination with other inducers. *Cancer Res*., **52**, 4634–4641.
28. Masuda,Y. *et al.* (1995) Bufalin induces apoptosis and influences the expression of apoptosis-related genes in human leukemia cells. *Leuk. Res*., **19**, 549–556.
29. Yu,C.H. *et al.* (2008) Apoptotic signaling in bufalin- and cinobufagin-treated androgen-dependent and -independent human prostate cancer cells. *Cancer Sci*., **99**, 2467–2476.
30. Jiang,Y. *et al.* (2010) Effects of bufalin on the proliferation of human lung cancer cells and its molecular mechanisms of action. *Cytotechnology*, **62**, 573–583.
31. Watabe,M. *et al.* (1997) Bcl-2 protein inhibits bufalin-induced apoptosis through inhibition of mitogen-activated protein kinase activation in human leukemia U937 cells. *Cancer Res*., **57**, 3097–3100.
32. Watabe,M. *et al.* (1998) Activation of AP-1 is required for bufalin-induced apoptosis in human leukemia U937 cells. *Oncogene*, **16**, 779–787.
33. Kurosawa,M. *et al.* (2001) Distinct PKC isozymes regulate bufalin-induced differentiation and apoptosis in human monocytic cells. *Am. J. Physiol. Cell Physiol*., **280**, C459–C464.
34. Li,H. *et al.* (2011) Na+/K+-ATPase α3 mediates sensitivity of hepatocellular carcinoma cells to bufalin. *Oncol. Rep*., **25**, 825–830.
35. Qi,F. *et al.* (2011) Bufalin and cinobufagin induce apoptosis of human hepatocellular carcinoma cells via Fas- and mitochondria-mediated pathways. *Cancer Sci*., **102**, 951–958.
36. Rabinowitz,J.D. *et al.* (2010) Autophagy and metabolism. *Science*, **330**, 1344–1348.
37. Klionsky,D.J. *et al.* (2000) Autophagy as a regulated pathway of cellular degradation. *Science*, **290**, 1717–1721.
38. Eisenberg-Lerner,A. *et al.* (2009) Life and death partners: apoptosis, autophagy and the cross-talk between them. *Cell Death Differ*., **16**, 966–975.
39. Maiuri,M.C. *et al.* (2007) Self-eating and self-killing: crosstalk between autophagy and apoptosis. *Nat. Rev. Mol. Cell Biol*., **8**, 741–752.
40. Turcotte,S. *et al.* (2010) Targeting cancer cells through autophagy for anticancer therapy. *Curr. Opin. Cell Biol*., **22**, 246–251.
41. Chen,S. *et al.* (2010) Autophagy is a therapeutic target in anticancer drug resistance. *Biochim. Biophys. Acta*, **1806**, 220–229.
42. Wang,K. *et al.* (2011) Quercetin induces protective autophagy in gastric cancer cells: involvement of Akt-mTOR- and hypoxia-induced factor 1α-mediated signaling. *Autophagy*, **7**, 966–978.
43. Shrivastava,A. *et al.* (2011) Cannabidiol induces programmed cell death in breast cancer cells by coordinating the cross-talk between apoptosis and autophagy. *Mol. Cancer Ther*., **10**, 1161–1172.

44. Brown,V.I. *et al.* (2003) Rapamycin is active against B-precursor leukemia *in vitro* and *in vivo*, an effect that is modulated by IL-7-mediated signaling. *Proc. Natl. Acad. Sci. U.S.A.*, **100**, 15113–15118.
45. Teachey,D.T. *et al.* (2006) The mTOR inhibitor CCI-779 induces apoptosis and inhibits growth in preclinical models of primary adult human ALL. *Blood*, **107**, 1149–1155.
46. Chen,G. *et al.* (2012) Mammalian target of rapamycin regulates isoliquiritigenin-induced autophagic and apoptotic cell death in adenoid cystic carcinoma cells. *Apoptosis*, **17**, 90–101.
47. Tirado,O.M. *et al.* (2005) Rapamycin induces apoptosis of JN-DSRCT-1 cells by increasing the Bax: Bcl-xL ratio through concurrent mechanisms dependent and independent of its mTOR inhibitory activity. *Oncogene*, **24**, 3348–3357.
48. Harada,H. *et al.* (2001) p70S6 kinase signals cell survival as well as growth, inactivating the pro-apoptotic molecule BAD. *Proc. Natl. Acad. Sci. U.S.A.*, **98**, 9666–9670.
49. Scott,R.C. *et al.* (2007) Direct induction of autophagy by Atg1 inhibits cell growth and induces apoptotic cell death. *Curr. Biol.*, **17**, 1–11.
50. Villanueva,A. *et al.* (2008) Pivotal role of mTOR signaling in hepatocellular carcinoma. *Gastroenterology*, **135**, 1972–1983.
51. Calvisi,D.F. *et al.* (2011) Increased lipogenesis, induced by AKT-mTORC1-RPS6 signaling, promotes development of human hepatocellular carcinoma. *Gastroenterology*, **140**, 1071–1083.

Received June 5, 2012; revised February 1, 2013; accepted February 4, 2013